Contributed paper

OPTO-ELECTRONICS REVIEW **11**(4), 297–304 (2003)

Fabrication of thin film polycrystalline CIS photovoltaic heterostructure

T. PISARKIEWICZ*, H. JANKOWSKI, E. SCHABOWSKA-OSIOWSKA, and L.J. MAKSYMOWICZ

Department of Electronics, AGH University of Science and Technology, 30 Mickiewicza Ave., 30-059 Cracow, Poland

Manufacturing processes and investigation of properties of thin film materials forming the $CuInSe_2$ (CIS) solar cell have been described. The cell consisted of the following layers: glass/ Mo/ p-$CuInSe_2$/ n-CdS/ n^+–ZnO/. CIS absorbers were obtained by pulse magnetron sputtering of metallic targets in argon yielding the multilayer precursors structures which were successively chalcogenised in selenium vapours. Cadmium sulfide buffer layer was manufactured by chemical bath deposition (CBD) method which offers the films with optimal properties. Window zinc oxide layers were obtained by RF magnetron sputtering of metallic Zn:Al target in oxygen reactive atmosphere. Thin film CIS solar cells with the efficiencies of the order of 6% have been produced. Further improvement in technology leading to CIS cells with better parameters have been discussed.

Keywords: chalcopyrite, $CuInSe_2$, thin film technology, solar cells.

1. Introduction

Thin film technologies are expected to substantially reduce manufacturing costs of solar cells due to the lowering of materials expenses and the deposition on large area substrates of a module size. Achievements in materials science and device development of compound semiconductors have led to impressively high efficiencies in the laboratory and in some cases to pilot production and manufacturing plants. CIS absorbers ($CuInSe_2$ and related quaternary compounds containing Ga called CIGS) are among the most promising photovoltaic materials. Chalcopyrite films in a polycrystalline form have resulted in solar cells with laboratory efficiencies exceeding 18% [1–3]. CIS solar cells show very good outdoor stability and radiation resistance [4]. The preparation method that yields the best laboratory efficiencies is coevaporation of all elements forming the chalcopyrite compound onto a heated substrate [1], but is difficult in upscaling.

Alternative techniques developed for fabrication of these cells are based on the two-stage processes that involve deposition of precursor metals and subsequent reaction with selenium (selenisation) to form $CuInSe_2$. The metal precursors can be deposited by more scalable and easier controlled procedures like evaporation [5,6], sputtering [7,8] and also non-vacuum processes [9]. Another alternative low cost technique is electrodeposition [10,11].

The authors developed sequential pulse magnetron sputtering in connection with chalcogenisation of metallic precursors in elemental Se [12–14]. This technique, avoiding the non-uniformity problems, seems to be perspective in industrial deposition of thin film solar cells. The optimisation of the deposition processes of CIS absorbers so far has been largely based on experiment. However, not only the reliable and accurate data but also the quantitative models for the chalcogenisation process are required. Establishing the limits for annealing times and temperatures, with securing at the same time the material properties of the CIS absorber, is at present important in terms of speed, thermal budget and costs of the solar cell.

2. Technology and properties of the CIS absorber

Absorber layer is the most important part of a solar cell. Absorbers in CIS cells are p-type semiconductors where the doping procedure is accomplished by deviation from stoichiometry. For the atomic ratio m = [Cu]/[In] slightly greater than 1, one obtains p-$CuInSe_2$. The concentration ratio of both metal atoms can be easily controlled in vacuum deposition of thin films. The control of Se content in the sample is more difficult and this is one of the reasons that coevaporation techniques give the best results.

2.1. Preparation of Cu/In multilayer precursors

In the technology developed by the authors, thin $CuInSe_2$ films were grown by selenisation of Cu-In alloys obtained from Cu/In metallic multilayers deposited by sputtering. The Cu/In multilayers were manufactured in one chamber

*e-mail: pisar@agh.edu.pl

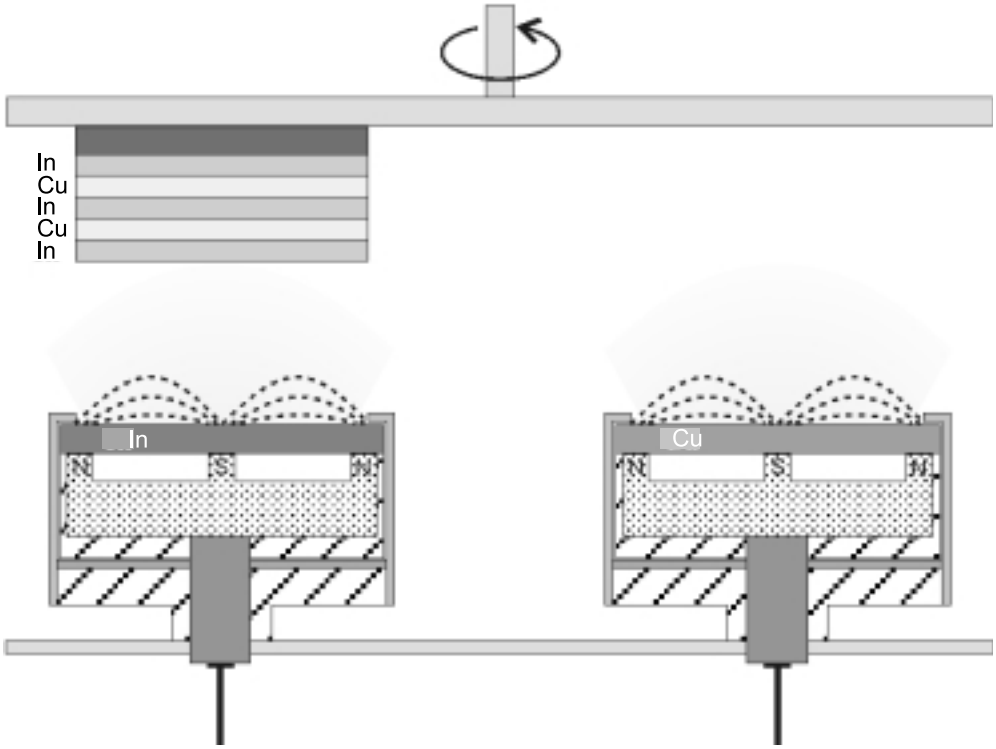

Fig. 1. Deposition of multilayer structure by magnetron sputtering of Cu and In targets.

from two independent Cu and In magnetron targets powered by pulse generators, Fig. 1.

The working chamber of the sputtering system was equipped with 4 magnetron targets of 10 cm in diameter each and rotating sample holder, enabling the deposition of multicomponent alloys, e.g., Cu-In-Ga. With the help of computer controller it was possible to deposit in one run multilayer structures with assumed thickness and composition and essentially by sequential deposition of Cu and In. Altogether 20 alternate layers with the size 5×5 cm^2 and total thickness varying from 250 to 500 nm were obtained, Fig. 2.

The elemental ratio was altered by adjusting the layer deposition time and in this case the atomic composition Cu/In varied from 2 to 0.5.

At the beginning of our investigations all multilayer structures deposited on float glass substrates were annealed at 300°C for 4 hrs in vacuum (ca 2 mPa) in a specially designed furnace to obtain the homogeneous alloys. Soon we observed that additional annealing is not mandatory and that the first step heating during selenisation process is sufficient.

2.2. Selenisation of precursors

All samples prepared by sputtering were selenised to obtain $CuInSe_2$. Due to the high toxicity of H_2Se, the selenisation of alloys was conducted using elemental Se. The samples were inserted into a partially closed graphite box containing selenium powder, Fig. 3.

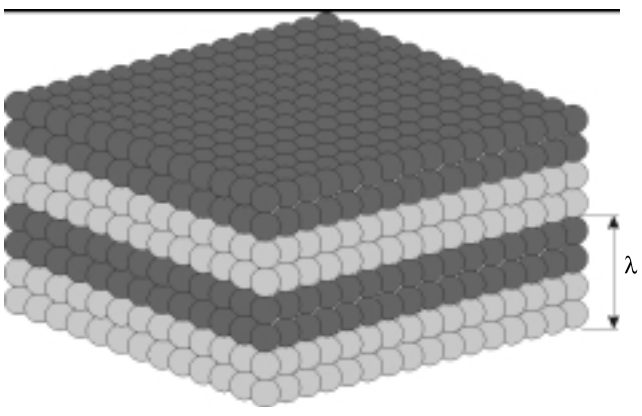

Fig. 2. Multilayer Cu/In structure.

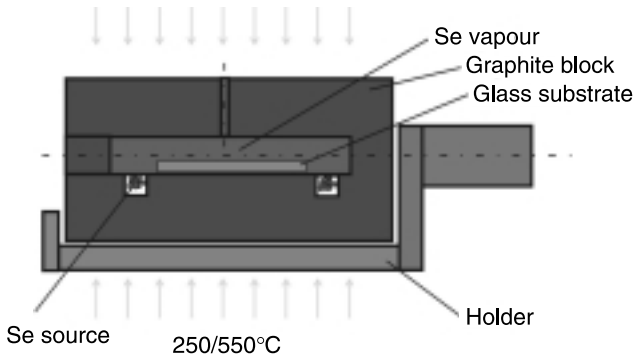

Fig. 3. The graphite container with sample holder and pots to accommodate the elemental Se. The spacing between the sample and the lid was kept low to ensure the overpressure of Se during selenisation.

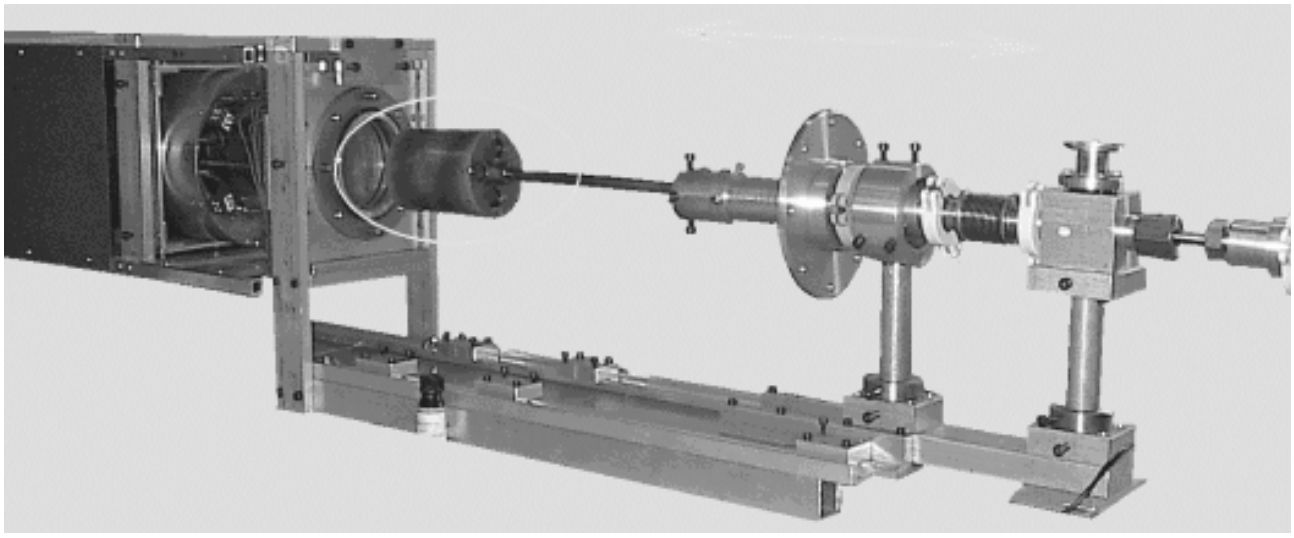

Fig. 4. Technological setup used for selenisation. The graphite container prepared for the loading of a new sample can be seen.

The box was then introduced into a quartz tube furnace evacuated to about 3 mPa by a mechanical pump. The quartz tube limited the dimensions of the sample but the diameter of the tube could be easily increased to scale-up the substrate size and to meet the demands of large-scale capacity. Outside view of the selenisation setup is shown in Fig. 4.

The process of selenisation was realized through two--step heating profile, Fig. 5. The first step at about 250°C enhanced the saturation of the alloy with selenium. At the second step for temperatures reaching 550°C chemical reactions and recrystallisation of the sample occurred. The total heating time varied up to about 1 hr.

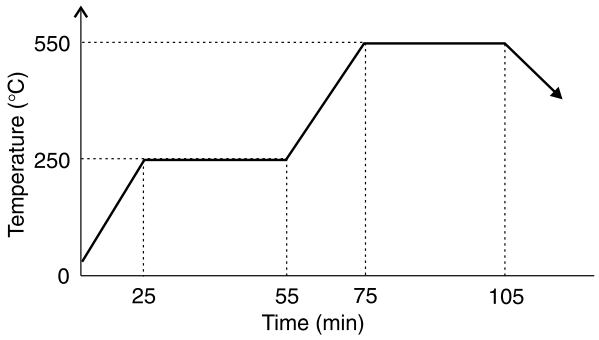

Fig. 5. Typical temperature profile during sample selenisation.

2.3. Properties of selenised samples

The obtained alloys and selenised CIS samples were examined with X-ray diffractometer Philips X'Pert MPD used for investigation of thin films. The XRD spectra were obtained in a parallel beam geometry and angle of incidence $\omega = 1°$ using Cu K_α radiation. The film morphology was determined by scanning electron microscopy (SEM) with additional measurements of fluorescence spectra.

XRD spectra for metallic precursor films deposited on molybdenum coated float glass (Mo constitutes the back electrode in the CIS solar cell structure) were identified as Cu_2In, CuIn, $Cu_{11}In_9$ or $CuIn_2$ intermetallic compounds, depending on the atomic composition and heating conditions. For In-rich samples the presence of phase not known for bulk alloys was observed [12] and was designated as $CuIn_2$ according to the results of work of Nakano *et al.* [15]. With the increase in Cu concentration, Figs. 6(a) and 6(b), the contents of CuIn and Cu_2In phases increase as can be expected. This observation is also confirmed by the results obtained by other authors [8].

The variation of Cu in the Cu-In alloy should influence the stoichiometry and homogeneity of CIS samples after selenisation. It is widely accepted [16] that during formation of $CuInSe_2$ semiconductor, on its surface the In-rich phase $CuIn_3Se_5$ is formed. The $CuIn_3Se_5$ phase is n-conductive and influences strongly the properties of the photovoltaic hetrojunction. XRD spectrum for nearly single-phase chalcopyrite $CuInSe_2$ sample obtained from stoichiometric Cu-In alloy by selenisation in the conditions as described above, is shown in Fig. 7. The preferential orientation of $CuInSe_2$ in (112) plane can be seen.

The small amount of CuSe phase is located on the film surface. This phase, which is detrimental to the film properties should be etched out. However, selecting carefully the selenisation conditions it is possible to obtain single phase $CuInSe_2$ film.

SEM micrographs of the film surface, Fig. 8, [17] for chalcogenised sample confirm the conclusions drawn from XRD measurements. Between the crystallites of CuSe on the surface of the film the crystallites of $CuInSe_2$ phase can be seen. This is also confirmed by elemental composition measurements. The good crystallinity of the $CuInSe_2$ phase can be associated with the increased Se vapour pressure what results from the construction of a graphite box.

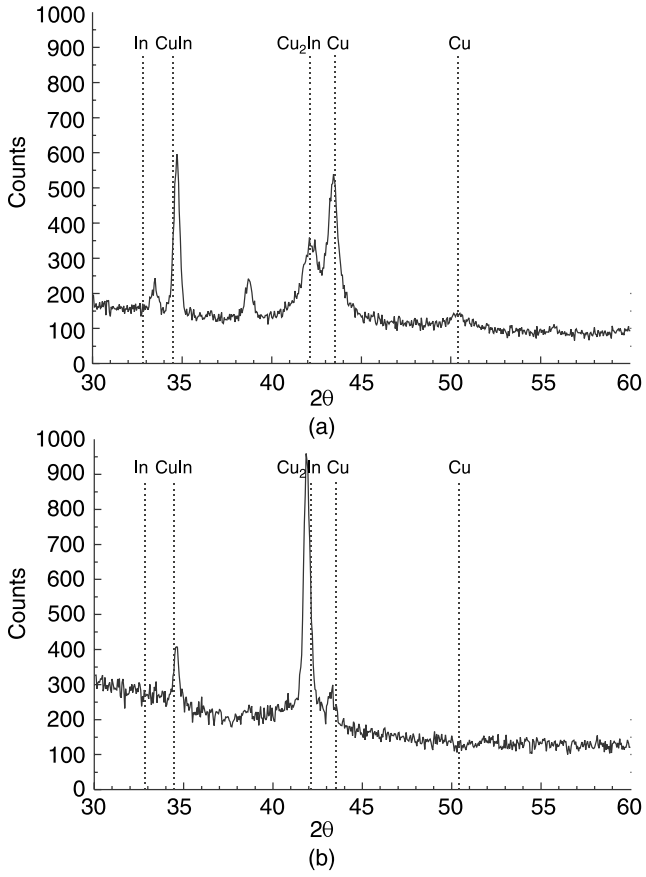

Fig. 6. Diffraction spectra for heat treated precursor alloys with Cu/In = 1 (a) and Cu/In = 2 (b).

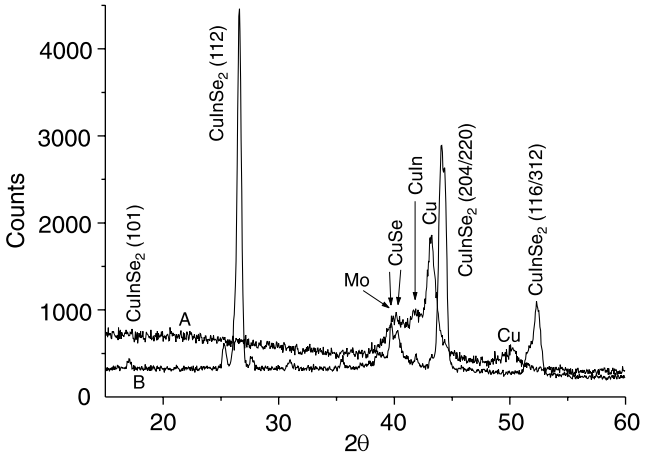

Fig. 7. Nearly single phase $CuInSe_2$ film with small amount of CuSe phase obtained by selenisation of the precursor with Cu/In = 1 in the graphite container; spectrum A – before selenisation, spectrum B – after selenisation.

3. Cadmium sulfide as a buffer layer in the cell structure

CIS absorbers need buffer layer to form photovoltaic heterojunction. One of the best buffer materials for this purpose is a thin (about 30 nm) CdS layer [16,18]. Cadmium sulphide is a wide bandgap semiconductor (E_g = 2.4 eV) and

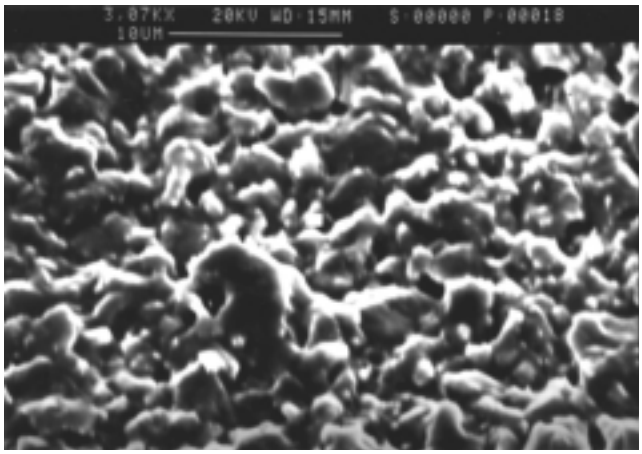

Fig. 8. The SEM micrograph showing the surface morphology of selenised sample from Fig. 7.

in a form of thin film is mostly obtained by vacuum methods. However, the highest efficiencies for n-CdS/p-CIS photovoltaic heterojunction are obtained with CdS manufactured by chemical bath deposition (CBD) method. The properties of that heterojunction are not fully understood yet and in particular it is not clear which role play the intrinsic properties of CdS, i.e. bandgap, band line up with CIS layer, lattice mismatch etc. It is also not clear which properties of CBD process (good step coverage, low temperature deposition, chemical passivation, lack of bombarding energetic species) influence the properties of the interface.

In some cases the superstrate-type CIS solar cells are made on glass coated previously by transparent conductive oxide [19]. In this case the tin oxide, indium tin oxide (ITO) or doped ZnO are covered by a layer of thin cadmium sulfide.

3.1. Chemical bath deposition technology

CdS films were grown by CBD technology using both uncoated glass (sodalime and Corning 7059) and glass plates covered by polycrystalline tin dioxide thin film [20]. This technology offers the deposition of a thin uniform film with a minimal thickness on the rough substrate surface. Deposition of CdS using uncoated glass substrates enabled optimisation of deposition parameters.

In CBD process three-stage chemical reactions lead to the formation of CdS:

- dissociation of cadmium complex and adsorption of Cd^{2+} on the substrate surface,
- hydrolysis of thiourea with production of S^{2-} ions,
- reaction of cadmium and sulfur ions with the formation of CdS.

The investigations of CdS growth have led the authors to the adoption of the following deposition conditions: concentration of cadmium sulfide 1 mM, of thiourea 100 mM and of ammonia 500 mM, and bath temperature 70°C. In the following, this technology was modified [21] and the

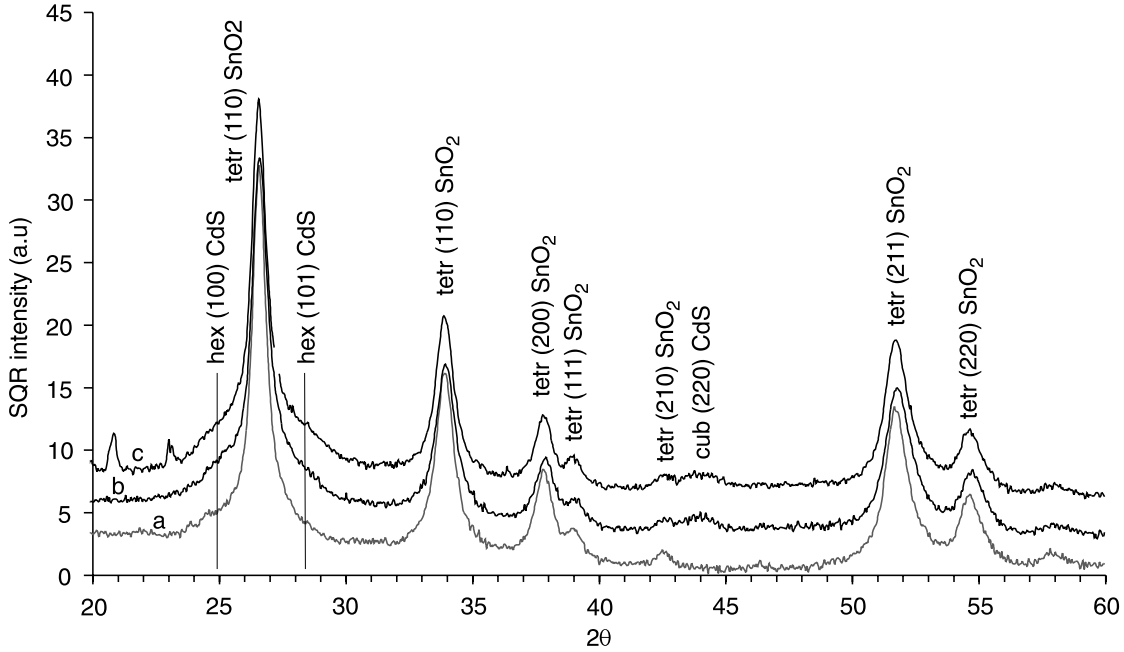

Fig. 9. X-ray diffraction spectra for SnO_2 (a) and CdS/SnO_2 bilayer before (c) and after (b) heat treatment.

solution consisted of 110 ml of deionised water with 73 mg $CdCl_2$, 2400 mg NH_4NO_3, 304 mg $CS(NH_2)_2$ and pH value was maintained in the range from 11.0 to 11.4.

Optical transmission measurements in the wavelength range 350–2200 nm have been performed, using Perkin-Elmer Lambda 19 spectrophotometer. X-ray diffraction spectra were obtained using Philips X'Pert MPD diffractometer. Surface topography investigations of CdS on glass and CdS/TCO bilayers were carried out with the help of atomic force microscope Digital Instruments NanoScope E SPM.

The as-grown and air-annealed (450°C, 2 hrs) samples have been studied to check the influence of heat-treatment on CBD CdS properties.

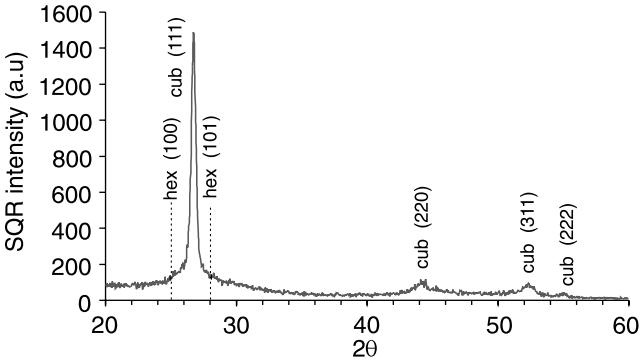

Fig. 10. X-ray diffraction spectrum for CdS on glass.

3.2. Properties of CdS films

X-ray diffraction spectra of the films manufactured by unmodified technology, Fig. 9, characterise both the substrate itself, i.e. polycrystalline tin dioxide, and the structure of CdS/SnO_2 bilayer. Tin dioxide reveals strong peaks of the tetragonal phase and no traces of the cubic phase were observed. For CdS the diffraction peaks of both hexagonal and cubic phases are possible but are screened by the more crystalline tin dioxide. The peak (220) for cubic CdS is clearly seen when the diffraction spectrum is shown in a narrower angle range. That peak is not affected by the heat treatment of CdS/SnO_2 bilayer and generally it follows from diffraction investigations that air annealing does not modify the CdS crystalline structure.

Diffraction spectrum for the film deposited by modified technology is shown in Fig. 10. In this case the CdS peaks are clearly seen, as there was no additional substrate layer. The cubic phase is dominant with preferred orientation in (111) plane.

AFM surface morphology investigations enable quantitative assessment of thin film surface parameters such as root mean square (RMS), or the average R_a roughness. It is also possible to determine the average grain size and inspect the film continuity. The AFM measurements were carried out in many locations of a given sample to minimise the statistical errors. The images of CdS grown on SnO_2 /glass substrate are shown in Fig. 11. As can be noticed SnO_2 sublayer influences morphology of deposited CdS film [20]. For CdS grown on glass the average grain size is about 30 nm and surface roughness parameters are RMS = 4 nm and R_a = 3 nm. For CdS grown on SnO_2/glass substrates the grain size is about 100 nm and roughness parameters are equal: RMS = 8 nm and R_a = 6 nm. The results of AFM measurements reported above are analogous to those of Martinez *et al*. [22] and indicate that CdS films reproduce morphology and roughness of the polycrystalline TCO sublayer.

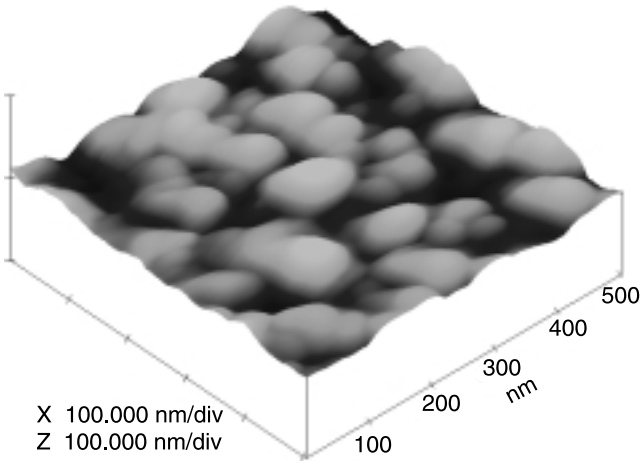

Fig. 11. AFM image of CdS film deposited onto SnO_2/glass substrate.

From the optical transmission spectra, Fig. 12, it can be deduced that the transmittance T of CdS deposited on Corning glass is not much less than that of the glass. The discrepancy occurs in the region below 500 nm, where the value of T starts to decrease due to interband absorption of light in CdS (further sudden decrease of T is caused by the absorption of UV light in glass). For CdS/SnO_2 bilayer structures the optical spectra are governed by the properties of tin dioxide, what is in agreement with measurements of Martinez *et al.* [22]. Annealing of the structure at 450°C causes the increase in transmittance of tin dioxide.

4. Technology of ZnO films

Zinc oxide thin film (E_g = 3.35 eV) plays in CIS solar cell the double role; a window layer transmitting the incident light generating photocarriers in the absorber and a contact layer enabling collection of the charge. For this purpose one deposits first a thin (50 nm) layer of undoped ZnO, and next a thicker layer (of the order of 1 μm) of n^+ – ZnO.

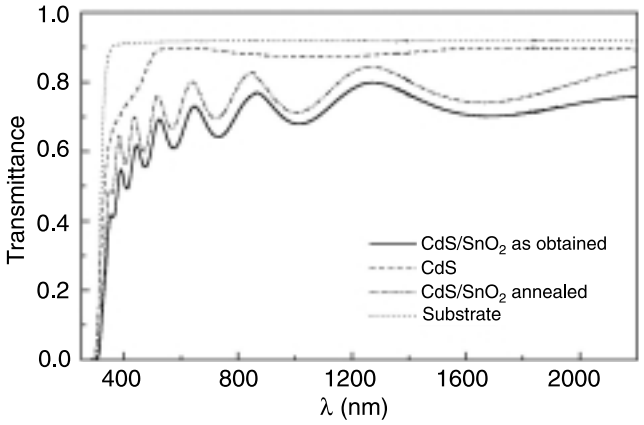

Fig. 12. Spectral dependence of transmittance for CdS and Cd/SnO_2 bilayer before and after heat treatment.

Recently thin films of ZnO have attracted interest as transparent conductive oxide (TCO) layers and in comparison to ITO are cheaper. Moreover in CIS solar cells are better energetically matched in the heterojunction than ITO. There have been reports of ZnO films prepared by spray pyrolysis, MOCVD, evaporation, pulsed laser deposition and magnetron sputtering. The most perspective technique enabling deposition onto large areas is sputtering [23]. Both DC sputtering from metallic Zn or Zn:2 wt.% Al as well as RF sputtering from pure oxide ZnO (or containing 2 wt% Al_2O_3) cathodes are developed. Although the best films are manufactured in RF sputtering, the high costs of oxide cathodes and low deposition rates indicate rather onto magnetron DC or MF (mid-frequency) sputtering.

Basing on literature reports and own technological experience the authors applied for deposition of ZnO films the technique of reactive magnetron sputtering of metallic targets with pulse voltage in the mid-frequency range. The conductivity of obtained samples was additionally controlled by the variation of O_2 concentration in the Ar + O_2 atmosphere.

The sputtering conditions were as follows:

- cathode: Zn:2 wt.% Al with 50 mm diameter
- substrate size: 5×5 cm
- substrate temp.: controlled in the range 100–200°C
- atmosphere: Ar + O_2
- working pressure: ca. 1 Pa
- power supply: Dora pulse power supply controlled in the range from 0.6 to 1.5 kW.

The lowest obtained resistivities of ZnO:Al thin films reached 5 Ω/square with the film thickness of the order of 1 μm. Undoped zinc oxide layers were not obtained. That technological simplification is often adopted in the industrial in-line deposition systems.

5. Properties of the photovoltaic heterostructure

The described technological processes enabled fabrication of the following structure: glass/ Mo/ p-$CuInSe_2$/ n-CdS/ n^+–ZnO/ Al which is shown in Fig. 13.

Average thicknesses of the constituting layers were as follows: Mo – 0.5 μm, CIS – 2.5 μm, CdS – 50 nm, ZnO – 1 μm, Al – 0.5 μm

The main parameters of a manufactured solar cell at illumination close to 100 mW/cm^2 were η = 6%, FF = 60%, V_{oc} = 450 mV, and j_{sc} = 25 mA/cm^2.

6. Conclusions

The parameters of the obtained photovoltaic heterostructure indicate that technological processes responsible for manufacturing of the constituting layers and absorber/buffer interface need to be optimised. In particular:

- in manufacturing of CIS absorber even trace concentrations of CuSe phase should be excluded what will improve the cell efficiency significantly,

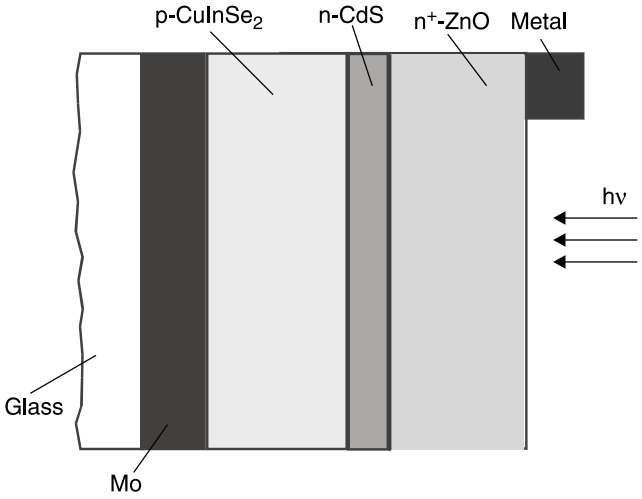

Fig. 13. Layer composition of the manufactured solar cell.

- the lower resistance of n^+– ZnO layer will result in the increase both in short circuit current j_{sc} and the fill factor *FF*,
- the absorber/buffer interface should have the expected phase composition with minimum concentration of defects.

In effect, the future selenisation process should be modified. The rapid thermal processing RTP of multilayer precursor with deposited additional Se layer instead of selenisation in Se vapours will allow the better control of Se concentration. Additionally this will improve the thermal budget of the process.

The change of composition of metallic precursor by adding a small amount of gallium will increase the absorber energy gap and in effect the open circuit voltage V_{oc} of the solar cell.

Acknowledgements

The authors gratefully acknowledge the financial support by the Polish Committee for Scientific Research under grant No. PBZ 05/T11/98.

References

1. M.A. Contreras, B. Egaas, K. Ramanathan, J. Hiltner, A. Schwartzlander, F. Hasoon, and R. Noufi, "Progress toward 20% efficiency in Cu(In,Ga)Se_2 polycrystalline thin-film solar cells", *Progress in Photovoltaics* **7**, 311–316 (1999).
2. T. Negami, Y. Hashimoto, and S. Nishiwaki, "Cu(In,Ga)Se_2 thin film solar cells with an efficiency of 18%", *Solar Energy Mater. Solar Cells* **67**, 331–335 (2001).
3. Y. Hagiwara, T. Nakada, and A. Kunioka, "Improved J_{sc} in CIGS thin films solar cells using a transparent conducting ZnO:B window layer", *Solar Energy Mater. Solar Cells* **67**, 267–271 (2001).
4. M. Yamaguchi, "Radiation resistance of compound semiconductor solar cells", *J. Appl. Phys.* **78**, 1476–1480 (1995).
5. A. Gupta and S. Isomura, "Precursor modification for preparation of CIS films by selenisation technique", *Solar Energy Mater. Solar Cells* **53**, 385–401 (1998).
6. J. Szot and U. Prinz, "Selenisation of metallic Cu-In thin films for $CuInSe_2$ solar cells", *J. Appl. Phys.* **66**, 6077–6083 (1989).
7. N.G. Dhere and K.W. Lynn, "$CuIn_{1-x}Ga_xSe_2$ thin film solar cells by two-selenisation processes using Se vapour", *Solar Energy Mater. Solar Cells* **41/42**, 271–279 (1996).
8. F.O. Adurodija, J. Song, S.D. Kim, S.H. Kwon, S.K. Kim, K.H. Yoon, and B.T. Ahn, "Growth of $CuInSe_2$ thin films by high vapour Se treatment of co-sputtered Cu-In alloy in a graphite container", *Thin Solid Films* **338**, 13–19 (1999).
9. G. Norsworthy, C.R. Leidholm, A. Halani, V.K. Kapur, R. Roe, B.M. Basol, and R. Matson, "CIS film growth by metallic ink coating and selenisation", *Solar Energy Mater. Solar Cells* **60**, 127–134 (2000).
10. R.N. Bhattacharya, W. Batchelor, and H. Wiesner, "14.1% $CuIn_{1-x}Ga_xSe_2$-based photovoltaic cells from electrodeposited precursors" *J. Electrochem. Soc.* **145**, 3435–3439 (1998).
11. A. Kampmann, V. Sittinger, J. Rechid, and R. Reineke-Koch, "Large area electrodeposition of Cu(In,Ga)Se_2", *Thin Solid Films* **361/362**, 309–313 (2000).
12. T. Pisarkiewicz, H. Jankowski, E. Schabowska-Osiowska, and L.J. Maksymowicz, "Growth of CIS layers using Cu-In alloys with optimised properties", *17th European Photovoltaic Solar Energy Conf.*, 22-26 October, Munich, 1221–1224 (2001).
13. T. Pisarkiewicz and H. Jankowski, "Vacuum selenisation of metallic multilayers for CIS solar cells", *Vacuum* **70**, 435–438 (2003).
14. H. Jankowski, T. Pisarkiewicz, C. Worek, and J. Stępiński, "Observation of selenisation process of $CuInSe_2$ thin films", *13th Int. Summer School Modern Surface Plasma Technology*, Mielno, 02-05 Sept., 277–280 (2002). (in Polish).
15. T. Nakano, T. Suzuki, N. Ohunaki, and S. Bata, "Alloying and electrical properties of evaporated Cu–In bilayer thin films", *Thin Solid Films* **334**, 192–195 (1998).
16. H.J. Lewerenz and H. Jungblut, *Photovoltaik,* Springer, Berlin, 1995. (in German).
17. T. Pisarkiewicz, H. Jankowski, and T. Stapiński, "Properties of CIS layers obtained by selenisation of Cu-In multilayer precursors", *Proc. International Conf. PV in Europe*, 7–11 Oct., Rome, 164–166 (2002).
18. W. Fuhs and R. Klenk, "Thin -film solar cells-overview", *Proc. 2nd World Conf. and Exhibition on Photovoltaic Solar Energy Conv.*, 6–10 July, Vienna, 381–386 (1998).
19. T. Nakada and T. Mise, "High-efficiency superstrate-type CIGS thin film solar cells with graded bangap absorber layers", *17th European Photovoltaic Solar Energy Conf.*, 22–26 October, Munich, 1027–1030 (2001).
20. T. Pisarkiewicz, E. Schabowska-Osiowska, E. Kusior, and A. Kowal, "Cadmium sulfide thin films manufactured by chemical bath deposition method", *J. Wide Bandgap Materials* **9**, 127–132 (2001).
21. E. Schabowska-Osiowska, T. Pisarkiewicz, T. Kenig, and B. Handke, "Cadmium sulfide thin films for photovoltaic applications", *27th Int. Conf. and Exhibition IMAPS Poland,* Podlesice-Gliwice, 16–19 Sept., 234–237 (2003).

22. M.A. Martinez, C. Guillen and J. Herrero, "Influence of the substrate nanostructure on the optical, structural and morphological properties of chemical bath deposited CdS thin films", *Proc. 2nd World Conf. and Exhibition on Photovoltaic Solar Energy Conv.*, 6–10 July, Vienna, 632–635 (1998).

23. J. Müller, G. Schöpe, O. Kluth, B. Rech, B. Szyszka, T. Höing, V. Sittinger, X. Jiang, G. Bräuer, R. Geyer, P. Lechner, H. Schade, and M. Ruske, "Large area mid-frequency magnetron sputtered ZnO films as substrates for silicon thin-film solar cells", *17th European Photovoltaic Solar Energy Conf.*, 22–26 October, Munich, 2876–2879 (2001).

